NANOMEDICINE

Fig. 4. Therapeutic effect of AEPO-liposomes on brain injury in the t-MCAO rats. The t-MCAO rats were injected via a tail vein with PBS or AEPO-liposomes immediately after the start of reperfusion. (as AEPO dosage of 8 μg/kg). Frozen sections of the brain in the t-MCAO model rats were prepared at 24 h after the injection of each sample, and then the sections were stained with TUNEL reagents and DAPI. The fluorescence images in the striatum (A) and the cortex (B) were observed by confocal laser scan microscopy. Quantitative data of apoptotic cerebral cells in the striatum (C) and the cortex (D) were obtained as the mean of 4 independent experiments. Solid columns indicate PBS control; and open columns, AEPO-liposomes. t-MCAO rats were injected via a tail vein with PBS, AEPO, AEPO-liposomes or PEGylated liposomes immediately after the start of reperfusion (as AEPO dosage of 8 μg/kg). E) The brains were dissected and stained with TTC at 24 h after the injection. Infarct volume (F) and the degree of brain swelling (G) were calculated by using Image J. Data are the mean ± S.D. (D, E; $n = 4$, G–H; $n = 7$). Significant differences are indicated as follows: $*p < 0.05$, $**p < 0.01$, $***p < 0.001$ as indicated by the brackets.
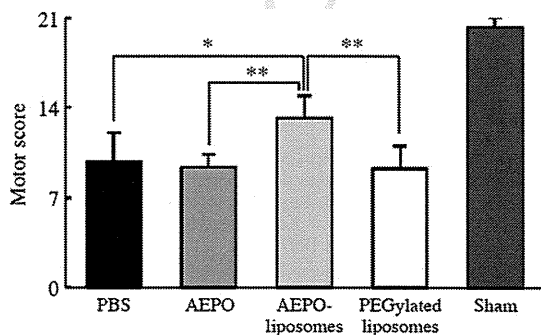

Fig. 5. Motor activity of t-MCAO model rats after treatment with AEPO-liposomes. t-MCAO model rats were injected via a tail vein with PBS, AEPO, AEPO-liposomes or PEGylated liposomes immediately after the start of reperfusion (as AEPO dosage of 8 μg/kg). At 24 h after the injection, the rats were assessed points in a 21-point neuropathological scoring system. Data are presented as the mean ± S.D. ($n = 7$). Significant differences are indicated as follows: $* p < 0.05$, $** p < 0.01$, $*** p < 0.001$ as indicated by the brackets.

We attempted to improve the outcome of cerebral stroke by enhancing the effect of low-dose (8 μg/kg) AEPO by using liposomal DDS technology. AEPO suppressed the infarct volume by approximately 30%, in contrast to the more than 70% achieved by the AEPO-liposomes. AEPO showed a cytoprotective effect on cerebral I/R injury via intravenous injection in spite of its short half-life in the bloodstream, probably because a brief exposure of neuronal cells to EPO is sufficient to cause a neuroprotective effect in vitro [19]. However, a long exposure to EPO is more effective than a short one for protecting neuronal cells [19]. AEPO-liposomes showed high accumulation and long retention in the ischemic hemisphere owing to a prolonged time in the blood circulation and the EPR effect. Therefore, we suggest that the significant neuroprotective effect of AEPO-liposomes should be attributed to the activation of many EPORs at the early stage after the start of reperfusion and to the long exposure of the cerebral cells to high concentration of AEPO.

Ischemic cerebral edema consists of cytotoxic edema and vasogenic edema resulting from dysfunction of the cellular osmotic pressure and disruption of the BBB, respectively. EPO has been shown to reduce astrocyte swelling by inhibiting the permeability of astrocyte aquaporin 4 after ischemia and also to protect neuronal cells possibly

through reducing cell swelling [34]. These findings suggest that AEPO might attenuate astrocyte swelling and neuronal cellular edema, resulting in suppression of neuronal cell death. In comparison with the other groups, the I/R rats treated with AEPO-liposomes significantly recovered neurological function (as assessed by motor score) at 24 h after an injection given immediately after the start of reperfusion. AEPO-liposomes mainly suppressed cerebral cell death in the striatum, which is the principal input nucleus of the basal ganglia receiving motor information from the cerebral motor cortex. Thus, the suppression of cell death in the striatum by the treatment with AEPO-liposomes resulted in the improvement of the motor abilities of the t-MCAO model rats. Nanoparticles appear to be suitable for delivering drugs in and around the striatum after cerebral ischemia, since the cerebral distribution of PEGylated liposomes corresponded to the region recovered by the treatment with AEPO-liposomes. This finding is of considerable interest as previous studies have found that some small molecular agents aid recovery mainly in the cerebral cortex [35,36]. Thus, a combination therapy using such agents together with liposomal drugs might be useful for the treatment of cerebral I/R injury. Our results indicate that AEPO-liposomes reduce progression of brain damage after recovery of blood flow from cerebral ischemia. AEPO-liposomes may be a useful adjunctive therapy after t-PA treatment in clinical practice.

5. Conclusions

The study has found that PEGylated liposomes injected immediately after reperfusion accumulated in the ischemic regions at an early stage after I/R and were retained there for at least 24 h after the start of reperfusion. Furthermore, AEPO-PEGylated liposomes significantly reduced cerebral I/R injury in t-MCAO model rats. Therefore, nanoparticles such as liposomes are potentially useful as a drug delivery carrier for the treatment of cerebral ischemia–reperfusion injury.

Acknowledgments

Appendix A. Supplementary data

Supplementary data to this article can be found online at doi:10.1016/j.jconrel.2012.02.004.

References

[1] Z.G. Zhang, L. Zhang, W. Tsang, H. Soltanian-Zadeh, D. Morris, R. Zhang, A. Goussev, C. Powers, T. Yeich, M. Chopp, Correlation of VEGF and angiopoietin expression with disruption of blood–brain barrier and angiogenesis after focal cerebral ischemia, J. Cereb. Blood Flow Metab. 22 (4) (2002) 379–392.

[2] Y. Yang, E.Y. Estrada, J.F. Thompson, W. Liu, G.A. Rosenberg, Matrix metalloproteinase-mediated disruption of tight junction proteins in cerebral vessels is reversed by synthetic matrix metalloproteinase inhibitor in focal ischemia in rat, J. Cereb. Blood Flow Metab. 27 (4) (2007) 697–709.

[3] A. Kastrup, K. Gröschel, T.M. Ringer, C. Redecker, R. Cordesmeyer, O.W. Witte, C. Terborg, Early disruption of the blood–brain barrier after thrombolytic therapy predicts hemorrhage in patients with acute stroke, Stroke 39 (8) (2008) 2385–2387.

[4] Z. Cheng, J. Zhang, H. Liu, Y. Li, Y. Zhao, E. Yang, Central nervous system penetration for small molecule therapeutic agents does not increase in multiple sclerosis- and Alzheimer's disease-related animal models despite reported blood–brain barrier disruption, Drug Metab. Dispos. 38 (2010) 1355–1361.

[5] H. Maeda, J. Wu, T. Sawa, Y. Matsumura, K. Hori, Tumor vascular permeability and the EPR effect in macromolecular therapeutics: a review, J. Control. Release 65 (1–2) (2000) 271–284.

[6] A.T. Perez, G.H. Domenech, C. Frankel, C.L. Vogel, Pegylated liposomal doxorubicin (Doxil) for metastatic breast cancer: the Cancer Research Network, Inc., experience, Cancer Invest. 20 (Suppl 2) (2002) 22–29.

[7] Y. Sato, K. Murase, J. Kato, M. Kobune, T. Sato, Y. Kawano, R. Takimoto, K. Takada, K. Miyanishi, T. Matsunaga, T. Takayama, Y. Niitsu, Resolution of liver cirrhosis using vitamin A-coupled liposomes to deliver siRNA against a collagen-specific chaperone, Nat. Biotechnol. 26 (4) (2008) 431–442.

[8] H. Epstein-Barash, D. Gutman, E. Markovsky, G. Mishan-Eisenberg, N. Koroukhov, J. Szebeni, G. Golomb, Physicochemical parameters affecting liposomal bisphosphonates bioactivity for restenosis therapy: internalization, cell inhibition, activation of cytokines and complement, and mechanism of cell death, J. Control. Release 146 (2) (2010) 182–195.

[9] J.M. Barichello, H. Handa, M. Kisyuku, T. Shibata, T. Ishida, H. Kiwada, Inducing effect of liposomalization on the transdermal delivery of hydrocortisone: creation of a drug supersaturated state, J. Control. Release 115 (1) (2006) 94–102.

[10] T.M. Allen, C. Hansen, Pharmacokinetics of stealth versus conventional liposomes: effect of dose, Biochim. Biophys. Acta 1068 (2) (1991) 133–141.

[11] Y. Gursoy-Ozdemir, A. Can, T. Dalkara, Reperfusion-induced oxidative/nitrative injury to neurovascular unit after focal cerebral ischemia, Stroke 35 (6) (2004) 1449–1453.

[12] J. Huang, U.M. Upadhyay, R.J. Tamargo, Inflammation in stroke and focal cerebral ischemia, Surg. Neurol. 66 (3) (2006) 232–245.

[13] M.D. Ginsberg, Current status of neuroprotection for cerebral ischemia: synoptic overview, Stroke 40 (3 Suppl) (2009) S111–S114.

[14] Effect of a novel free radical scavenger, edaravone (MCI-186), on acute brain infarction. Randomized, placebo-controlled, double-blind study at multicenters, Cerebrovasc. Dis. 15 (3) (2003) 222–229.

[15] A. Hishida, Clinical analysis of 207 patients who developed renal disorders during or after treatment with edaravone reported during post-marketing surveillance, Clin. Exp. Nephrol. 11 (4) (2007) 292–296.

[16] L. Hoyte, J. Kaur, A.M. Buchan, Lost in translation: taking neuroprotection from animal models to clinical trials, Exp. Neurol. 188 (2) (2004) 200–204.

[17] M. Brines, A. Cerami, Emerging biological roles for erythropoietin in the nervous system, Nat. Rev. Neurosci. 6 (6) (2005) 484–494.

[18] P. Ghezzi, M. Brines, Erythropoietin as an antiapoptotic, tissue-protective cytokine, Cell Death Differ. 11 (Suppl 1) (2004) S37–S44.

[19] E. Morishita, S. Masuda, M. Nagao, Y. Yasuda, R. Sasaki, Erythropoietin receptor is expressed in rat hippocampal and cerebral cortical neurons, and erythropoietin prevents in vitro glutamate-induced neuronal death, Neuroscience 76 (1) (1997) 105–116.

[20] M. Buemi, C. Caccamo, L. Nostro, E. Cavallaro, F. Floccari, G. Grasso, Brain and cancer: the protective role of erythropoietin, Med. Res. Rev. 25 (2) (2005) 245–259.

[21] A.L. Sirén, M. Fratelli, M. Brines, C. Goemans, S. Casagrande, P. Lewczuk, S. Keenan, C. Gleiter, C. Pasquali, A. Capobianco, T. Mennini, R. Heumann, A. Cerami, H. Ehrenreich, P. Ghezzi, Erythropoietin prevents neuronal apoptosis after cerebral ischemia and metabolic stress, Proc. Natl. Acad. Sci. U. S. A. 98 (7) (2001) 4044–4049.

[22] X. Yu, J.J. Shacka, J.B. Eells, C. Suarez-Quian, R.M. Przygodzki, B. Beleslin-Cokic, C.S. Lin, V.M. Nikodem, B. Hempstead, K.C. Flanders, F. Costantini, C.T. Noguchi, Erythropoietin receptor signalling is required for normal brain development, Development 129 (2) (2002) 505–516.

[23] C. Savino, R. Pedotti, F. Baggi, F. Ubiali, B. Gallo, S. Nava, P. Bigini, S. Barbera, E. Fumagalli, T. Mennini, A. Vezzani, M. Rizzi, T. Coleman, A. Cerami, M. Brines, P. Ghezzi, R. Bianchi, Delayed administration of erythropoietin and its non-erythropoietic derivatives ameliorates chronic murine autoimmune encephalomyelitis, J. Neuroimmunol. 172 (1–2) (2006) 27–31.

[24] S. Erbayraktar, G. Grasso, A. Sfacteria, Q.W. Xie, T. Coleman, M. Kreilgaard, L. Torup, T. Sager, Z. Erbayraktar, N. Gokmen, O. Yilmaz, P. Ghezzi, P. Villa, M. Fratelli, S. Casagrande, M. Leist, L. Helboe, J. Gerwein, S. Christensen, M.A. Geist, L.Ø. Pedersen, C. Cerami-Hand, J.P. Wuerth, A. Cerami, M. Brines, Asialoerythropoietin is a nonerythropoietic cytokine with broad neuroprotective activity in vivo, Proc. Natl. Acad. Sci. U. S. A. 100 (11) (2003) 6741–6746.

[25] X. Wang, C. Zhu, X. Wang, J.G. Gerwien, A. Schrattenholz, M. Sandberg, M. Leist, K. Blomgren, The nonerythropoietic asialoerythropoietin protects against neonatal hypoxia-ischemia as potently as erythropoietin, J. Neurochem. 91 (4) (2004) 900–910.

[26] H. Nagasawa, K. Kogure, Correlation between cerebral blood flow and histologic changes in a new rat model of middle cerebral artery occlusion, Stroke 20 (8) (1989) 1037–1043.

[27] A.J. Hunter, J. Hatcher, D. Virley, P. Nelson, E. Irving, S.J. Hadingham, A.A. Parsons, Functional assessments in mice and rats after focal stroke, Neuropharmacology 39 (5) (2000) 806–816.

[28] D. Vaudry, P.J. Stork, P. Lazarovici, L.E. Eiden, Signaling pathways for PC12 cell differentiation: making the right connections, Science 296 (5573) (2002) 1648–1649.

[29] T.H. Lee, H. Kato, S.T. Chen, K. Kogure, Y. Itoyama, Expression of nerve growth factor and trkA after transient focal cerebral ischemia in rats, Stroke 29 (8) (1998) 1687–1696 discussion 1697.

[30] J.P. Yang, X.F. Liu, H.J. Liu, G.L. Xu, Y.P. Ma, Extracellular signal-regulated kinase involved in NGF/VEGF-induced neuroprotective effect, Neurosci. Lett. 434 (2) (2008) 212–217.

[31] T. Ishii, T. Asai, T. Urakami, N. Oku, Accumulation of macromolecules in brain parenchyma in acute phase of cerebral infarction/reperfusion, Brain Res. 1321 (2010) 164–168.

[32] Recommendations for standards regarding preclinical neuroprotective and restorative drug development, Stroke 30 (12) (1999) 2752–2758.

[33] M. Yemisci, Y. Gursoy-Ozdemir, A. Vural, A. Can, K. Topalkara, T. Dalkara, Pericyte contraction induced by oxidative-nitrative stress impairs capillary reflow despite successful opening of an occluded cerebral artery, Nat. Med. 15 (9) (2009) 1031–1037.

[34] E. Gunnarson, Y. Song, J.M. Kowalewski, H. Brismar, M. Brines, A. Cerami, U. Andersson, M. Zelenina, A. Aperia, Erythropoietin modulation of astrocyte water permeability as a component of neuroprotection, Proc. Natl. Acad. Sci. U. S. A. 106 (5) (2009) 1602–1607.

[35] S.W. Jang, M. Okada, I. Sayeed, G. Xiao, D. Stein, P. Jin, K. Ye, Gambogic amide, a selective agonist for TrkA receptor that possesses robust neurotrophic activity, prevents neuronal cell death, Proc. Natl. Acad. Sci. U. S. A. 104 (41) (2007) 16329–16334.

[36] S. Amemiya, T. Kamiya, C. Nito, T. Inaba, K. Kato, M. Ueda, K. Shimazaki, Y. Katayama, Anti-apoptotic and neuroprotective effects of edaravone following transient focal ischemia in rats, Eur. J. Pharmacol. 516 (2) (2005) 125–130.

NANOMEDICINE
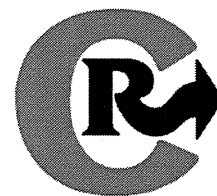
Development of anti-HB-EGF immunoliposomes for the treatment of breast cancer

Kaoru Nishikawa [a], Tomohiro Asai [a], Hirokazu Shigematsu [a], Kosuke Shimizu [a], Hisakazu Kato [b], Yoshihiro Asano [b], Seiji Takashima [b], Eisuke Mekada [c], Naoto Oku [a], Tetsuo Minamino [b,*]

[a] Department of Medical Biochemistry and Global COE Program, School of Pharmaceutical Sciences, University of Shizuoka, 52-1 Yada, Suruga-ku, Shizuoka 422-8526, Japan
[b] Department of Cardiovascular Medicine, Osaka University Graduate School of Medicine, Suita, Osaka 565-0871, Japan
[c] Department of Cell Biology, Research Institute for Microbial Diseases, Osaka University, Suita, Osaka 565-0871, Japan

ARTICLE INFO

ABSTRACT

Increased expression of heparin-binding epidermal growth factor-like growth factor (HB-EGF) is frequently observed in certain cancers such as ovarian and breast cancers, and this protein is a desirable target for drug delivery by a drug delivery system (DDS). In the present study, we developed novel immunoliposomes targeting HB-EGF for cancer therapy. The immunoliposomes significantly associated with Vero-H cells overexpressing HB-EGF compared with their binding to wild-type Vero cells, whereas liposomes without modification by the antibody did not associate with either type of cells. Moreover, enhanced uptake of the immunoliposomes into Vero-H cells was observed as well as that into MDA-MB-231 human breast cancer cells, which are known to highly express HB-EGF. These results suggest that HB-EGF mediates the binding and uptake of the immunoliposomes in HB-EGF-expressing cells. Next, we determined the therapeutic effect of these immunoliposomes encapsulating an anticancer drug on tumor-bearing mice. For this purpose, we prepared doxorubicin (DOX)-encapsulated immunoliposomes and injected them intravenously into mice bearing MDA-MB-231 cancer cells. As a result, these DOX-encapsulated immunoliposomes suppressed not only tumor progression but also tumor regression. In conclusion, our results indicate that anti-HB-EGF antibody-modified liposomes could be a useful DDS carrier for the treatment of HB-EGF-expressing cancers.

© 2011 Elsevier B.V. All rights reserved.

1. Introduction

Heparin-binding epidermal growth factor-like growth factor (HB-EGF) is known to stimulate the growth of various cells in an autocrine or a paracrine manner. This protein is highly expressed on various cancer cells, such as those of ovarian and breast cancer [1,2], and is also expressed on tumor angiogenic vessels [3,4]. Therefore, HB-EGF seems to be a target molecule for the treatment of certain cancers. In fact, CRM197, which binds to the EGF-domain of HB-EGF and prevents HB-EGF from binding to ErbB receptors and therefore regulates the cell proliferation, is now under clinical trials [5]. The usefulness of HB-EGF as a molecular target of cancer treatment has been suggested in several reviews [6–8]. Although HB-EGF can be produced as a membrane-anchored form (proHB-EGF) and later processed to its soluble form, a significant amount of proHB-EGF remains on the cell surface [9]. Therefore, HB-EGF might be also a useful target molecule for drug delivery via a DDS to tumors and tumor angiogenic vessels.

In the present study, we aimed at delivering an anticancer drug to HB-EGF-expressing cancer cells by use of liposomes as a drug carrier. Polyethylene glycol (PEG)-modified liposomes have been the most widely investigated as carriers of drugs and molecules having biological activities, since PEG forms an aqueous layer on the liposomal surface that avoids reticuloendothelial system (RES) trapping of the liposomes [10,11]. PEGylated liposomes have a relatively long circulation time and tend to accumulate in tumor tissues through leaky angiogenic vessels, a phenomenon referred to as the enhanced permeability and retention (EPR) effect [12,13]. Moreover, liposomalization can reduce off-target toxicity of the drugs encapsulated [14]. In fact, PEG-modified liposomes containing doxorubicin (DOX) have been used in clinical cancer therapy. On the other hand, actively targeted liposomes decorated with ligands such as antibodies [15,16], proteins such as transferrin [17], and peptides [18–20] achieve more selective drug delivery to tumor tissues. These ligands that recognize tumor- or tumor angiogenic vessel-associated molecules are conjugated to the head of the PEG-chain of liposomes.

Herein, we decorated DOX-loaded liposomes with anti-HB-EGF antibody and evaluated the systemic and targeted delivery of DOX to cancer cells in breast cancer-bearing mice. The results indicate that this immunoliposomal DOX significantly suppressed tumor growth in comparison with non-modified PEG-liposomal DOX. Our findings suggest that targeted delivery of anti-HB-EGF-modified

PEGylated liposomes could be a useful carrier of doxorubicin for the treatment of HB-EGF-expressing cancers.

2. Materials and Methods

2.1. Materials

Anti-human HB-EGF monoclonal antibody (IgG) was ordered and received from Medical and Biological Laboratories Co. Ltd. The monoclonal antibody clone 3E9 specific for HB-EGF was obtained by the method described previously [21]. The 3E9 clone recognized the EGF-like domain of human proHB-EGF, but not that of mouse proHB-EGF. Hydrogenated soy phosphatidylcholine (HSPC), methoxy-polyethyleneglycol 2000-conjugated distearoylphosphatidylethanolamine (DSPE-PEG), and cholesterol were gifts from Nippon Fine Chemical Co. Ltd. (Kobe, Japan). DSPE-PEG-maleimide (SUNBRIGHT DSPE-0.20MA) was obtained from NOF Co. Ltd. (Tokyo, Japan). 1,1'-Dioctadecyl- 3,3,3',3',-tetramethylindocarbocyanine perchlorate (DilC$_{18}$) was purchased from Molecular Probes, Inc. (Eugene, OR).

2.2. Preparation of Fab' of anti-HB-EGF monoclonal antibody

Stock solution of anti-HB-EGF IgG was applied onto a PD-10 column (GE Healthcare, UK., Ltd., Buckinghamshire) to exchange the solvent for 100 mM sodium citrate buffer, pH 3.5 (100 mg IgG/20 mL). To eliminate the Fc region of the IgG, pepsin (from porcine gastric mucosa, Sigma-Aldrich) solution (final concentration of 0.01% w/v) was added to the antibody solution and incubated the mixture at 37 °C for 3 h, after which the reaction was stopped by the addition of a 10% volume of 3 M Tris–HCl (pH 7.5). The generated F(ab')$_2$ was washed twice with 100 mM sodium phosphate buffer, pH 6.0, and concentrated by ultrafiltration (5,000 g for 20 min) with an Amicon® Ultra-4 (10,000 NMWL, Millipore). Ten milligrams aliquot of F(ab)'$_2$ was diluted with 100 mM sodium phosphate buffer, and 0.1 mL of 100 mM cysteamine hydrochloride was added to a final volume of 1 mL, followed by incubation at 37 °C for 90 min. Then, the reaction solution was purified by gel-filtration chromatography (1.0 cm×50 cm, Ultrogel AcA, PALL Life Sciences), and the Fab' fraction was collected with a fraction collector. The Fab' fraction was concentrated by ultrafiltration (5,000 g for 30 min) with Amicon Ultra-4 (10,000 NMWL).

2.3. Preparation of plain liposomes

Liposomes were prepared by thin lipid-film hydration followed by vortexing and sonication. In brief, 20 µmol HSPC and 10 µmol cholesterol dissolved in chloroform were transferred to a round-bottomed flask, evaporated until a thin lipid film had formed on a rotary evaporator under reduced pressure, and stored in vacuo for at least 1 h. The dried film was hydrated with 2 mL of saline, warmed at 65 °C in a water bath, vortexed until the lipids had become detached from the side of the flask, and sonicated with a bath-type sonicator at 65 °C. Three cycles of the following were performed: freezing of the liposomal solution in the flask with liquid nitrogen, thawing at room temperature, incubating at 65 °C in a water bath for 5 min, and vortexing for 30 s. Then, the liposomes were filtered through polycarbonate membrane filters having 100-nm-diameter pores by use of an Extruder (Lipex, Vancouver) at 65 °C. Finally, the liposome solution was diluted with saline; and the liposomal pellet was collected after ultracentrifugation (450,000 g×1 h, CS120GXL, Hitachi) and resuspended in 2 mL of saline.

For the fluorescence-labeling of liposomes, HSPC, cholesterol, and DilC$_{18}$ (2:1:0.1 as a molar ratio) dissolved in chloroform were used for preparing a thin lipid film. Further preparation was essentially the same as described above except that all procedures were done under shading from ambient light.

For the encapsulation of DOX into the liposomes, the thin lipid film was hydrated in 250 mM ammonium sulfate (pH 5.5) instead of saline; and after freeze-thawing, extrusion for sizing, and centrifugation, the liposomes resuspended in saline was incubated in the presence of 1.8 mg/mL DOX at 65 °C for 1 h. Untrapped DOX was removed by ultracentrifugation, and the liposomal pellet was resuspended in saline (final concentration of 10 mM as DSPC). The encapsulation efficiency of DOX was calculated based on the amount of untrapped DOX and liposomal DOX after the addition of Triton X-100, with DOX quantified at 484-nm absorbance.

2.4. Surface decoration of liposomes with PEG or anti-HB-EGF antibody-PEG

DSPE-PEG (MPEG-2000-DSPE) and DSPE-PEG-maleimide were dissolved in saline to a final concentration of 10 mM each. One milliliter of plain liposomes (10 mM as DSPC) prepared as described above were incubated at 65 °C for 15 min after addition 100 µL of DSPE-PEG or DSPE-PEG-maleimide to obtain PEG-modified liposomes (PEG-Lip) and PEG-maleimide-modified liposomes.

The coupling of Fab' with the maleimide moiety of PEG-maleimide-modified liposomes was performed according to the method described previously [22], with the following modification: Fab' and PEG-maleimide-modified liposomes (1:1 molar ratio of Fab' and maleimide moiety) were mixed, and the coupling reaction was carried out at 4 °C for 20 h. Excess Fab' was separated from the Fab'-coupled liposomes by use of Sepharose 4 Fast Flow gel filtration, and the liposomal fraction was collected. After ultracentrifugation at 450,000 g, 4 °C for 1 h (CS120GXL, Hitachi), the liposomal pellet was resuspended in 1 mL of saline.

Liposome size and ζ-potential were determined with a Zeta Sizer (Nano –ZS, Malvern Instruments, Worcs, UK).

2.5. Cells and cell culture

Vero cells derived from African green monkey's kidney were cultured in MEM medium (GIBCO) supplemented with 10% fetal bovine serum (FBS; Sigma-Aldrich), 100 units/mL penicillin G (MP Biomedicals, Irvine, CA), and 100 µg/mL streptomycin (MP Biomedicals) in a CO$_2$ incubator. Vero-H cells isolated by transfection with human HB-EGF cDNA [23] were cultured similarly except that the medium was supplemented with 1 µg/mL G418.

MDA-MB-231 human breast cancer cells were cultured in Leibovitz L-15 medium (GIBCO) supplemented with 10% FBS, 100 units/mL penicillin G, and 100 µg/mL streptomycin in a CO$_2$ incubator.

2.6. Real-time PCR

Vero, Vero-H, and MDA-MB-231 cells were cultured on a 60-mm culture dish for 24 h and washed with ice-cold PBS for three times. Then, the cells were collected by a scraper; and total RNA was extracted with RNeasy Plus Mini Kit (QIAGEN) according to the manufacturer's instruction. Then cDNA was generated from the total RNA samples (4 µg) by using a Ready-To-Go T-Primed First-Strand Kit (GE Healthcare). In the presence of human HB-EGF or β-actin primer (Takara Bio Inc. Shiga, Japan), and SYBR Premix Ex Taq II (Takara Bio), real-time PCR was performed with a Thermal Cycler Dice Real Time System (Takara Bio). The PCR conditions were the following: 95 °C for 30 sec, followed by 40 cycles of 95 °C for 5 sec, 60 °C for 30 sec; 95 °C for 15 sec, 60 °C for 30 sec, and 95 °C for 15 sec.

2.7. Western blotting

Vero, Vero-H, and MDA-MB-231 cells were cultured on a 60-mm culture dish for 24 h and washed with ice-cold PBS for three times. Then, the cells were solubilized in lysis buffer (50 mM Tris–HCl [pH7.4] containing 1% Triton-X, 150 mM NaCl, and protease inhibitors [2 mM PMSF, 50 µg/mL aprotinin, 50 µg/mL pepstatin, and 0.2 mM

leupeptin]). The supernatant of the cell lysate was collected and suspended in loading buffer (16 mM Tris–HCl, 2.5% glycerol, 0.5% SDS, 200 mM 2-mercaptoethanol, 0.001% bromophenol blue; pH 6.8). Immediately after having been heated at 95 °C for 5 min, the sample was subjected to reducing SDS-PAGE on 10% acrylamide gel. Protein concentrations were measured by using a BCA Protein Assay Reagent Kit (PIERCE Biotechnology, Rockford, IL).

After separation by SDS-PAGE, proteins were transferred electrophoretically (40 V, 90 min) to a PVDF membrane (Bio-Rad). After having been blocked with 3% BSA in TBS/Tween 20 buffer (TBS/T: 50 mM Tris HCl [pH 7.4] containing 150 mM NaCl and 0.05% Tween 20), the blots were incubated at 25 °C for 1 h with goat polyclonal anti-HB-EGF antibody (1:2,000 solution, R&D systems) for the detection of HB-EGF. The membrane was washed thrice with TBS/T, and was probed for 60 min at 25 °C with donkey anti-goat horseradish peroxidase-conjugated secondary antibody (1:4,000 dilution). The probed membranes were washed 3 times (10 min each time) with TBS/T, and immunoreactive proteins were detected by using the enhanced chemiluminescence method.

2.8. Binding to and uptake of Ab-PEG-Lip into various cells

Vero, Vero-H, and MDA-MB-231 cells were cultured in a 24-well plate (2×10^4 cells/500 μL/well) at 37 °C for 48 h. After removal of the medium, DiIC$_{18}$-labeled PEG-Lip or Ab-labeled PEG-Lip (0.05 to 0.2 mM as DSPC) was added to the well; and the cells were then incubated at 4 °C or 37 °C. Next, the cells were washed thrice with cold PBS and solubilized with 10 mM Tris buffer, pH 7.4, containing 0.1% SDS. The samples were diluted 200-fold with 10 mM Tris buffer, pH 7.4, containing 0.1% SDS; and aliquots were transferred to a 96-well black plate. The fluorescence intensity was monitored with a multiplate reader (Infinite M200, Tecan), with excitation and emission wave lengths of 549 nm and 592 nm, respectively. The amount of DiIC$_{18}$ associated with the cells was calculated from the standard curve.

2.9. Cell proliferation assay

MDA-MB-231 cells were seeded (2×10^4 cells/well) into a 24-well plate and incubated overnight in a CO$_2$ incubator. After a change of the medium, the cells were incubated at 37 °C for 4 h in the presence of DOX-encapsulated anti-HB-EGF-decorated immunoliposomes (Ab-PEG-LipDOX), DOX-encapsulated PEG-liposomes (PEG-LipDOX) or free DOX. Then, the viability of the cells was measured with TetraColorOne™ (Seikagaku, Tokyo, Japan) according to the manufacturer's instruction.

2.10. Therapeutic experiment

MDA-MB-231 cells were subcutaneously implanted (8×10^6 cells/ 0.2 mL/mouse) into 17-week-old BALB/C nu/nu female mice (Japan SLC Inc., Shizuoka, Japan). Then, saline (control), PEG-LipDOX or Ab-PEG-LipDOX was intravenously injected once a week for 3 weeks, on days 14, 21, and day 28 after tumor implantation. The amount of DOX injected was 10 mg/kg each time and; therefore, a total of 30 mg/kg DOX was injected. The tumor size and body weight were monitored daily from day 12 after tumor implantation. Tumor volume was calculated from the following formula:

Tumor volume $= 0.4 \times a$
$$\times b^2 (a; \text{largest diameter}, b; \text{smallest diameter})$$

The animals were cared for according to the Animal Facility Guidelines of the University of Shizuoka. All animal experiments were approved by the Animal and Ethics Committee of the University of Shizuoka.

Table 1
Particle size and ζ-potential of liposomes.

Liposomes	Size (nm)	ζ-potential (mV)
PEG-Lip	136	-0.03
PEG-LipDOX	139	-3.30
Ab-PEG-Lip	134	-3.02
Ab-PEG-LipDOX	142	-2.94

2.11. Statistical analysis

Differences between groups were evaluated by analysis of variance (ANOVA) with the Tukey post-hoc test.

3. Results

3.1. Characterization of Ab-PEG-Lip and Ab-PEG-LipDOX

At first, we examined the characteristics of anti-HB-EGF antibody-modified liposomes (Ab-PEG-Lip) and DOX-loaded Ab-PEG-Lip (Ab-PEG-LipDOX). As shown in Table 1, all liposomal preparations showed similar sizes, about 140 nm, and had almost neutral charges. The efficiency of conjugation of the Fab' fragment of anti-HB-EGF antibody to liposomal PEG-maleimide was determined by the protein amount before and after the conjugation reaction. When 1.94 mg Fab' had been applied on the liposomes, 1.31 mg Fab' was recovered in the
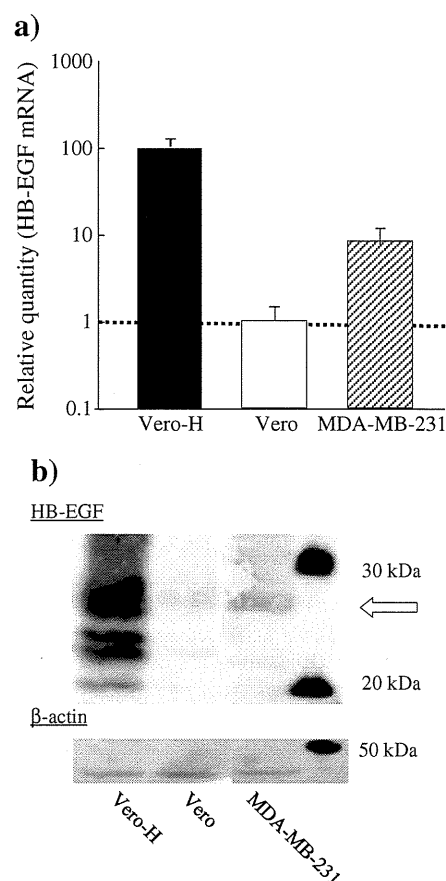

Fig. 1. Expression of HB-EGF and its transcript in various cell lines. a) Relative expression of HB-EGF mRNA was determined by real-time PCR. Total RNA was extracted from Vero, Vero-H, and MDA-MB-231 cells; and then real-time PCR for HB-EGF and β-actin was performed as described in Materials and Methods. b) Western blotting was performed on Vero, Vero-H, and MDA-MB-231 cells. The arrow indicates the position of HB-EGF. Total proteins (14 μg/sample) were fractionated by 10% SDS-PAGE. Following electrophoresis, the proteins were transferred to a PVDF membrane, and Western blotting was performed as described in Materials and Methods.
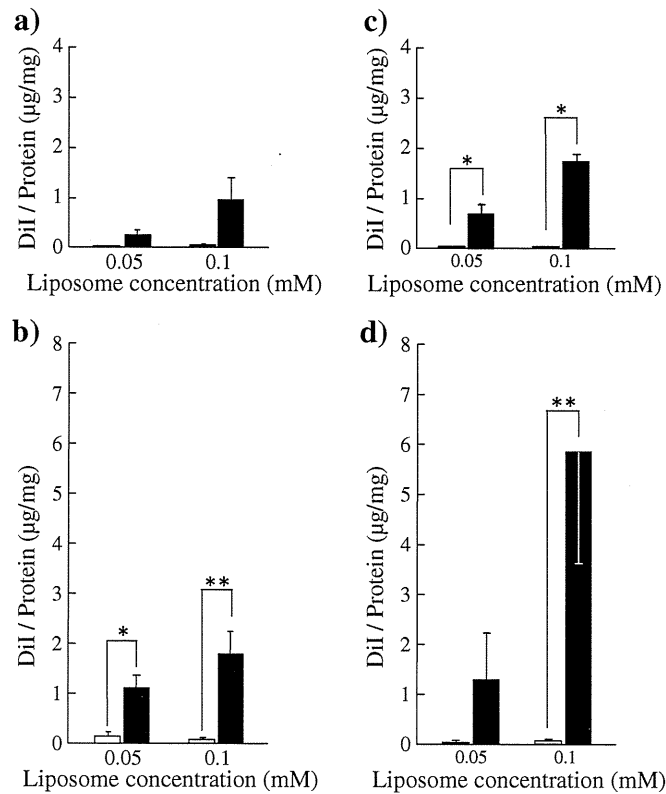
Fig. 2. Binding to and uptake of anti-HB-EGF antibody-modified liposomes into Vero and Vero-H cells. DilC$_{18}$-labeled PEG-Lip (open columns) and Ab-PEG-Lip (closed columns) were incubated with Vero (a, c) or Vero-H (b, d) cells at 4 °C (a, b) or at 37 °C (c, d) for 4 h. The amount of liposomes bound to Vero or Vero-H cells was determined fluorometrically. Liposomes bound to Vero or Vero-H cells are presented as the amount of DilC$_{18}$ per amount of cellular protein. Data show the mean values and S.D. (n = 3). Significant differences are shown with asterisks: * $p < 0.05$ and **$p < 0.01$, as indicated by the brackets or *versus* corresponding value for PEG-Lip.

liposomal fraction, indicating that the conjugation efficiency was about 67%. The encapsulation efficiency of DOX in PEG-LipDOX and Ab-PEG-LipDOX was 88.2 ± 6.9% and 88.4 ± 4.3%, respectively. These data indicate that the conjugation of Fab' to liposomes and DOX loading were successfully achieved.

3.2. Binding to and uptake of anti-HB-EGF immunoliposomes by HB-EGF-expressing cells

Before examining the cellular-association aspect of Ab-PEG-Lip, we assessed the expression levels of HB-EGF on Vero cells, Vero-H cells, and MDA-MB-231 cells by performing real-time PCR and Western blotting. Quite high expression of HB-EGF on Vero-H cells was confirmed by both real-time PCR (Fig. 1a) and Western blotting (Fig. 1b). Also, substantial amounts of HB-EGF mRNA and protein were expressed on MDA-MB-231 cells. In the case of Vero cells, the expression level of HB-EGF mRNA was about 100-fold less than that in Vero-H cells; and only a light band was detected by Western blotting.

The association of Ab-PEG-Lip with Vero, Vero-H, and MDA-MB-231 cells was examined for evaluating the targeting effectiveness of the liposomes. Ab-PEG-Lip bound more to Vero-H cells than to Vero cells (Fig. 2a, b). Moreover, the amount of the immunoliposomes taken up into cells was greater for Vero-H cells than for Vero cells. Most of the liposome-associated label (Dil) had probably been taken up into the cells at 37 °C, although some of it may have remained bound to the surface of the cells.

Next the uptake of Ab-PEG-Lip into human breast cancer cells was investigated by using MDA-MB-231 cells, which had been confirmed by real-time PCR and Western blotting (Fig. 1) to have high expression of HB-EGF protein. Ab-PEG-Lip was significantly taken up into the MDA-MB-231 cells at 37 °C(Fig. 3). These data would also include the liposomes bound to the cells. Therefore, these immunoliposomes bound to and were

taken up specifically into the HB-EGF-expressing breast-cancer cells, indicating that they could be a useful carrier for drug delivery.

3.3. Antiproliferative effect of DOX encapsulated in anti-HB-EGF immunoliposomes on HB-EGF-expressing cells

Next, the anti-proliferative effect of DOX encapsulated in Ab-PEG-Lip on MDA-MB-231 cells as well as on Vero-H cells was examined. As shown in Fig. 4, the immunoliposomal formulation of DOX suppressed the growth of both MDA-MB-231 and Vero-H cells in a
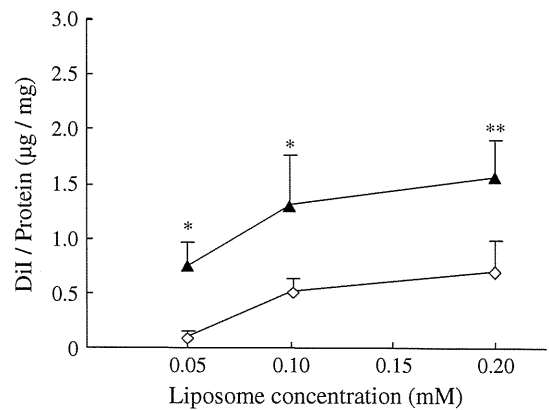

Fig. 3. Association of anti-HB-EGF antibody-modified liposomes with MDA-MB-231 cells. MDA-MB-231 cells were incubated with DilC$_{18}$-labeled PEG-Lip (◊) or Ab-PEG-Lip (▲) at 37 °C for 4 h. After the cells had been washed with PBS, the amount of liposomes associated with them was determined fluorometrically. Amounts of bound/internalized liposomes are presented as the amount of DilC$_{18}$ per amount of MDA-MB-231 cell protein. Data show the mean values and S.D. (n = 3). Significant differences are shown with asterisks: * $p < 0.05$ and ** $p < 0.01$ *versus* corresponding value for PEG-Lip.
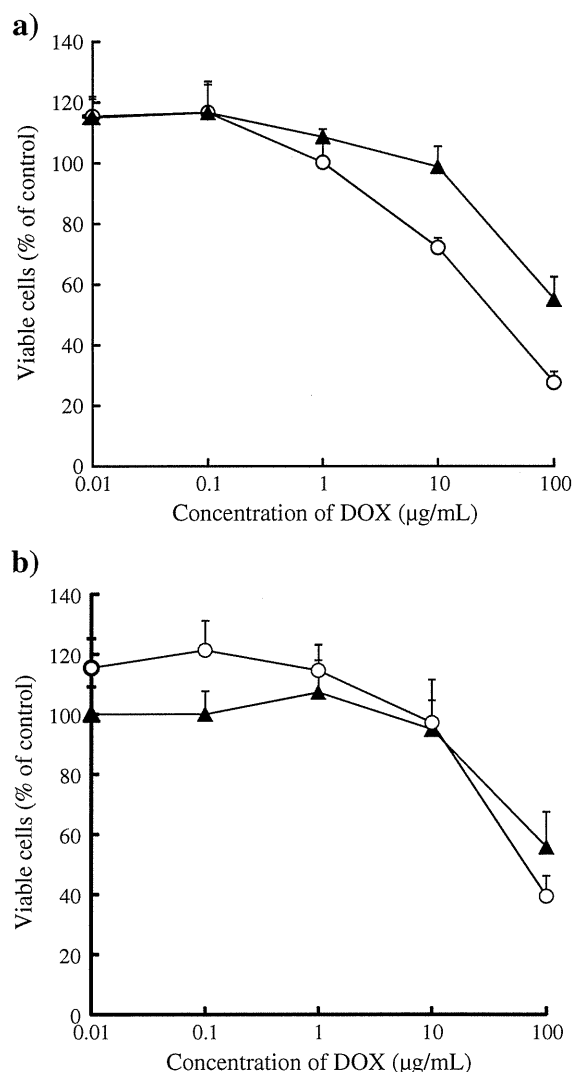
a)

b)

Fig. 4. Anti-proliferative effect of Ab-PEG-LipDOX on Vero-H and MDA-MB-231 cells. Vero-H (a) or MDA-MB-231(b) cells (2.5 x 10³ cells/well) were seeded into a 96-well plate. Ab-PEG-LipDOX (▲) or free DOX (O) was added at the indicated concentrations (0.01, 0.1, 1, 10, and 100 μg/mL as DOX), and the cells were then incubated for 4 h at 37 °C. After having been washed with PBS, the cells were cultured in fresh medium for an additional 48 h at 37 °C. TetraColor ONE™ was then added to each well. After a 3-h incubation, the absorbance at 450 nm was measured. Data (n = 4) are presented as the percentage (mean and S.D.) of viable cells relative to the control (taken as 100%) at the indicated DOX dosages.

dose-dependent manner. Although free DOX suppressed the growth of both types of cells a little stronger than liposomal DOX, Ab-PEG-LipDOX might be expected to be effective *in vivo*. Since PEG-Lip did not show comparable association with the cells, we did not examine the effect of DOX encapsulated in PEG-Lip.

3.4. Therapeutic efficacy of DOX encapsulated in anti-HB-EGF immunoliposomes on MDA-MB-231 tumor-bearing mice

Finally, the therapeutic effect of DOX-encapsulated immunoliposomes on MDA-MB-231 solid tumors implanted subcutaneously into mice was examined. As shown in Fig. 5, both PEG-LipDOX and Ab-PEG-LipDOX strongly suppressed the tumor growth when give as 3 doses of 10 mg/kg DOX. Free DOX of this amount could not be injected due to the severe side effects. Between liposomal DOX-treated groups, PEG-LipDOX-treated group showed only a little tumor growth and the Ab-PEG-LipDOS-treated group showed tumor regression. The change in body weight was monitored as an indicator of side effects, and a decrease in body weight was observed in both liposomal DOX-treated
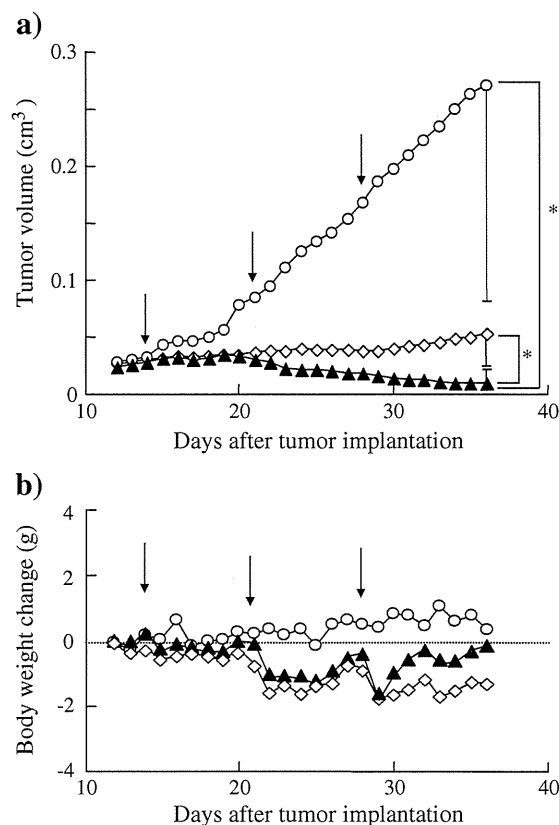
a)

b)

Fig. 5. Suppression of tumor growth in MDA-MB-231 carcinoma-bearing mice treated with Ab-PEG-LipDOX. BALB/C nu/nu female mice (n = 5) were implanted subcutaneously with MDA-MB-231 carcinoma into the left posterior flank. At 14, 21, and 28 days after tumor implantation, they were injected intravenously with PEG-LipDOX (◊), Ab-PEG-LipDOX (▲) or saline (O). The injected dose of liposomal DOX was 10 mg/kg as DOX for each administration. Tumor volume (a) and change in body weight (b) of the tumor-bearing mice were monitored daily after day 12. Data in "a" are presented as the mean tumor volume and S.D., where the S.D. bars are shown only for the last points for the sake of graphic clarity. Arrows show the day of treatment. Asterisks indicate a significant difference: * $p < 0.05$, as indicated by the brackets.

groups. This decrease, however, was not so much; and the body weight recovered at least by a week after the last treatment (Fig. 5b).

4. Discussion

In spite of diagnostic and therapeutic advances, cancer is still the leading cause of death in many countries. The present study focused on the treatment of human cancers by use of a HB-EGF-targeted liposomal drug delivery system, since various cancerous cells are known to frequently express this protein. For this purpose, we developed anti-HB-EGF antibody-decorated PEG liposomes encapsulating DOX. In this study, we used Fab' antibody instead of IgG, since removal of the Fc region endows antibody-decorated liposomes with a relatively long circulation time in the bloodstream by avoiding RES trapping [24]. In the present protocol, the efficiency of Fab' conjugation to the liposomal surface was about 70%, which amount was calculated to represent about 120 μg protein/μmol lipids. Since about 30 μg Fab'/μmol lipids is reported to be necessary for the function of immunoliposomes [25,26], the Ab-PEG-Lip prepared presently displayed a sufficient amount of Fab'. The size of liposomes is another important factor for deciding the pharmacokinetics of the liposomes, and about 140-nm liposomes are considered desirable for their accumulation in tumor tissue by the EPR effect [27].

Firstly the expression of HB-EGF in Vero, Vero-H, and MDA-MB-231 cells was examined at mRNA and protein levels. Extremely high expression of HB-EGF was observed in Vero-H cells that had been

constructed for overexpressing human HB-EGF. Vero cells, which are non-cancerous normal cells originally isolated from an African green monkey, also expressed HB-EGF; although the mRNA expression level was about 100-fold less than that of Vero-H cells, and 10-fold less than that of MDA-MB-231 cells. Since the anti-human HB-EGF antibody used for Western blotting is known to cross react with monkey HB-EGF, an HB-EGF band was detected in Vero cells.

By use of these cells, we determined the binding to and uptake of Ab-EGF-Lip into the cells. The cell-associated liposomes detected after incubation at 4 °C might have been mainly due to liposomes bound on the surface of the cells, whereas those detected after incubation at 37 °C would have included both bound and internalized liposomes. The binding of Ab-EGF-Lip to Vero H and MDA-MB-231 cells was very obvious compared with that to Vero cells, although Ab-EGF-Lip also bound to Vero cells to some extent. This finding suggests that the expression of endogenous HB-EGF in Vero cells was adequate for binding of the liposomes to some extent. Alternatively, part of the binding might be explained by non-specific binding of Ab-EGF-Lip via the Fab' despite its specificity. Since PEG-Lip showed little association with those cells, the anti-HB-EGF Fab'-decoration could have been responsible for the increased association of Ab-EGF-Lip with them.

DOX encapsulation into Ab-PEG-Lip was performed by the remote loading method using ammonium sulfate, since this method enables stable entrapment of DOX in the internal aqueous phase of PEG-liposomes [28] and immunoliposomes [29]. When the antiproliferative effect of Ab-PEG-LipDOX was examined, the cytotoxicity of Ab-PEG-LipDOX against Vero-H and MDA-MB-231 cells was found to be comparable to that of free DOX.

Finally, we performed a therapeutic experiment by use of MDA-MB-231 breast cancer cell-bearing mice. Both PEG-LipDOX and Ab-PEG-LipDOX strongly suppressed tumor growth. PEG-liposomes are known to accumulate in tumor tissues due to the EPR effect. Since this effect in tumor tissues is based on the leaky angiogenic vessels, hyper vascular tumors such as breast and ovarian tumors are desired targets. Therefore, PEG-liposomes encapsulating DOX were originally used for the treatment of ovarian and breast cancers and of HIV-associated Kaposi's sarcoma. The strong *in vivo* therapeutic effect of PEG-LipDOX against MDA-MB-231 tumors observed in this study is thus reasonable. Moreover, Ab-PEG-LipDOX, having both passive and active targeting characteristics, showed a stronger therapeutic effect against MDA-MB-231 tumors than PEG-LipDOX. PEG-liposomes that accumulate in tumor tissues after an intravenous injection are thought to reside mainly in the interstitial spaces in the tumor. On the other hand, decoration of them with some specific probes may alter the intratumoral distribution of the liposomes, and increase the uptake of liposomal drugs into the target cells, as observed in the present study.

As shown in Fig. 5, tumor growth inhibition was similar in both PEG-LipDOX- and Ab-PEG-LipDOX-treated groups until day 20, and differential therapeutic effect between targeted and non-targeted liposomes became obvious after second and third injection of them. We do not know the reason why the advantage of immunoliposomes was not obvious until day 20 at present. One possible explanation is as follows: The growth of MDA-MB-231 cells in vivo was not so fast, and the tumor mass was quite small at the first injection time, namely day 14. Therefore, the angiogenesis that produced leaky endothelium did not hardly occur. Moreover immune system would be still quite active that eliminate even PEGylated liposomes at this stage. In fact, although both PEG-LipDOX and Ab-PEG-LipDOX suppressed tumor growth to some extent compared to control, body weight change was not so obvious compared to that after second and third injection. At the time of second and third injection, immune systems were weakened because of tumor residing that helps the accumulation of liposomes in the tumor by EPR effect through neovessels. Since extravasation by EPR effect is prerequisite for the active targeting of immunoliposomes to the tumor cells, Ab-PEG-LipDOX thus accumulated in the

interstitial space of the tumor interacted with tumor cells and produced higher therapeutic effect than PEG-LipDOX. Actually, tumor was hardly palpated in two mice out of five after the third treatment with Ab-PEG-LipDOX.

5. Conclusions

For the purpose of active targeting of anticancer drugs to cancer cells, anti-HB-EGF antibody-decorated liposomes were prepared. These immunoliposomes bound to and were taken up into not only Vero-H cells highly expressing HB-EGF but also MDA-MB-231 human breast cancer cells. Moreover, DOX-encapsulated, anti-HB-EGF antibody-decorated liposomes caused strong suppression and regression of MDA-MB-231 tumors in mice. These results indicate that anti-HB-EGF antibody-decorated liposomes could be a useful DDS carrier for the treatment of HB-EGF-expressing cancers.

References

[1] S. Miyamoto, M. Hirata, A. Yamazaki, T. Kageyama, H. Hasuwa, H. Mizushima, Y. Tanaka, H. Yagi, K. Sonoda, M. Kai, H. Kanoh, H. Nakano, E. Mekada, Heparin-binding EGF-like growth factor is a promising target for ovarian cancer therapy, Cancer Res. 64 (2004) 5720–5727.

[2] S. Miyamoto, H. Yagi, F Yotsumoto, S. Horiuchi, T. Yoshizato, T. Kawarabayashi, M. Kuroki, E. Mekada, New approach to cancer therapy: heparin binding-epidermal growth factor-like growth factor as a novel targeting molecule, Anticancer Res. 27 (2007) 3713–3721.

[3] P.P. Ongusaha, J.C. Kwak, A.J. Zwible, S. Macip, S. Higashiyama, N. Taniguchi, L. Fang, S.W. Lee, HB-EGF is a potent inducer of tumor growth and angiogenesis, Cancer Res. 64 (2004) 5283–5290.

[4] V.B. Mehta, G.E. Besner, HB-EGF promotes angiogenesis in endothelial cells via PI3-kinase and MAPK signaling pathways, Growth Factors 25 (2007) 253–263.

[5] S. Miyamoto, H. Yagi, F. Yotsumoto, T. Kawarabayashi, E. Mekada, Heparin-binding epidermal growth factor-like growth factor as a novel targeting molecule for cancer therapy, Cancer Sci. 97 (2006) 341–347.

[6] S. Miyamoto, T. Fukami, H. Yagi, M. Kuroki, F. Yotsumoto, Potential for molecularly targeted therapy against epidermal growth factor receptor ligands, Anticancer Res. 29 (2009) 823–830.

[7] H. Tsujioka, F. Yotsumoto, K. Shirota, S. Horiuchi, T. Yoshizato, M. Kuroki, S. Miyamoto, Emerging strategies for ErbB ligand-based targeted therapy for cancer, Anticancer Res. 30 (2010) 3107–3112.

[8] H. Tsujioka, F. Yotsumoto, S. Hikita, T. Ueda, M. Kuroki, S. Miyamoto, Targeting the heparin-binding epidermal growth factor-like growth factor in ovarian cancer therapy, Curr. Opin. Obstet. Gynecol. 23 (2011) 24–30.

[9] S. Higashiyama, H. Iwabuki, C. Morimoto, M. Hieda, H. Inoue, N. Matsushita, Membrane-anchored growth factors, the epidermal growth factor family: beyond receptor ligands, Cancer Sci. 99 (2008) 214–220.

[10] D.D. Lasic, Doxorubicin in sterically stabilized liposomes, Nature 380 (1996) 561–562.

[11] Y. Sadzuka, A. Nakade, R. Hirama, A. Miyagishima, Y. Nozawa, S. Hirota, T. Sonobe, Effects of mixed polyethyleneglycol modification on fixed aqueous layer thickness and antitumor activity of doxorubicin containing liposome, Int. J. Pharm. 238 (2002) 171–180.

[12] Y. Matsumura, H. Maeda, A new concept for macromolecular therapeutics in cancer chemotherapy: mechanism of tumoritropic accumulation of proteins and the antitumor agent smancs, Cancer Res. 46 (1986) 6387–6392.

[13] H. Maeda, Y. Matsumura, EPR effect based drug design and clinical outlook for enhanced cancer chemotherapy, Adv. Drug Deliv. Rev. 63 (2011) 129–130.

[14] A. Gabizon, H. Shmeeda, Y. Barenholz, Pharmacokinetics of pegylated liposomal doxorubicin: review of animal and human studies, Clin. Pharmacokinet. 42 (2003) 419–436.

[15] A.S. Manjappa, K.R. Chaudhari, M.P. Venkataraju, P. Dantuluri, B. Nanda, C. Sidda, K.K. Sawant, R.S. Murthy, Antibody derivatization and conjugation strategies: application in preparation of stealth immunoliposome to target chemotherapeutics to tumor, J. Control. Release 150 (2011) 2–22.

[16] K. Atobe, T. Ishida, E. Ishida, K. Hashimoto, H. Kobayashi, J. Yasuda, T. Aoki, K. Obata, H. Kikuchi, H. Akita, T. Asai, H. Harashima, N. Oku, H. Kiwada, In vitro efficacy of a sterically stabilized immunoliposomes targeted to membrane type 1 matrix metalloproteinase (MT1-MMP), Biol. Pharm. Bull. 30 (2007) 972–978.

[17] R. Suzuki, T. Takizawa, Y. Kuwata, M. Mutoh, N. Ishiguro, N. Utoguchi, A. Shinohara, M. Eriguchi, H. Yanagie, K. Maruyama, Effective anti-tumor activity of oxaliplatin encapsulated in transferrin-PEG-liposome, Int. J. Pharm. 346 (2008) 143–150.

[18] N. Maeda, Y. Takeuchi, M. Takada, Y. Sadzuka, Y. Namba, N. Oku, N, Antineovascular therapy by use of tumor neovasculature-targeted long-circulating liposome, J. Control. Release 100 (2004) 41–52.

[19] Y. Katanasaka, T. Ida, T.T. Asai, N. Maeda, N. Oku, Effective delivery of an angiogenesis inhibitor by neovessel-targeted liposomes, Int. J. Pharm. 360 (2008) 219–224.

[20] Y. Katanasaka, T. Ishii, T. Asai, H. Naitou, N. Maeda, F. Koizumi, S. Miyagawa, N. Ohashi, N. Oku, Cancer antineovascular therapy with liposome drug delivery systems targeted to BiP/GRP78, Int. J. Cancer 127 (2010) 2685–2698.

[21] M. Hamaoka, I. Chinen, T. Murata, S. Takashima, R. Iwamoto, E. Mekada, Anti-human HB-EGF monoclonal antibodies inhibiting ectodomain shedding of HB-EGF and diphtheria toxin binding, J. Biochem. 148 (2010) 55–69.

[22] T. Ishida, D.L. Iden, T.M. Allen, A combinatorial approach to producing terically stabilized (Stealth) immunoliposomal drugs, FEBS Lett. 460 (1999) 129–133.

[23] K. Goishi, S. Higashiyama, M. Klagsbrun, N. Nakano, T. Umata, M. Ishikawa, E. Mekada, N. Taniguchi, Phorbol ester induces the rapid processing of cell surface heparin-binding EGF-like growth factor: conversion from juxtacrine to paracrine growth factor activity, Mol. Biol. Cell 6 (1995) 967–980.

[24] K. Maruyama, N. Takahashi, T. Tagawa, K. Nagaike, M. Iwatsuru, Immunoliposomes bearing polyethyleneglycol-coupled Fab' fragment show prolonged circulation time and high extravasation into targeted solid tumors in vivo, FEBS Lett. 413 (1997) 177–180.

[25] C. Mamot, D.C. Drummond, U. Greiser, K. Hong, D.B. Kirpotin, J.D. Marks, J.W. Park, Epidermal growth factor receptor (EGFR)-targeted immunoliposomes mediate specific and efficient drug delivery to EGFR- and EGFRvIII-overexpressing tumor cells, Cancer Res. 63 (2003) 3154–3161.

[26] C. Mamot, D.C. Drummond, C.O. Noble, V. Kallab, Z. Guo, K. Hong, D.B. Kirpotin, J.W. Park, Epidermal growth factor receptor-targeted immunoliposomes significantly enhance the efficacy of multiple anticancer drugs in vivo, Cancer Res. 65 (2005) 11631–11638.

[27] N. Oku, Y. Tokudome, T. Asai, H. Tsukada, Evaluation of drug targeting strategies and liposomal trafficking, Curr. Pharm. Des. 6 (2000) 1669–1691.

[28] G. Haran, R. Cohen, L.K. Ba, Y. Barenholz, Transmembrane ammonium sulfate gradients in liposomes produce efficient and stable entrapment of amphipathic weak bases, Biochim. Biophys. Acta 1151 (1993) 201–215.

[29] N. Emanuel, E. Kedar, E.M. Bolotin, N.I. Smorodinsky, Y. Barenholz, Preparation and characterization of doxorubicin-loaded sterically stabilized immunoliposomes, Pharm. Res. 13 (1996) 352–359.

Sex Differences in Neointimal Hyperplasia Following Endeavor *Zotarolimus*-Eluting Stent Implantation

Daisaku Nakatani, MD, PhD, Junya Ako, MD, PhD, Jennifer A. Tremmel, MD, MS, Katsuhisa Waseda, MD, PhD, Hiromasa Otake, MD, PhD, Bon-Kwon Koo, MD, PhD, Akiyoshi Miyazawa, MD, Yoichiro Hongo, MD, Seung-Ho Hur, MD, PhD, Ryota Sakurai, MD, Paul G. Yock, MD, Yasuhiro Honda, MD, and Peter J. Fitzgerald, MD, PhD*

Inconsistent results in outcomes have been observed between the genders after drug-eluting stent implantation. The aim of this study was to investigate gender differences in neointimal proliferation for the Endeavor zotarolimus-eluting stent (ZES) and the Driver bare-metal stent (BMS). A total of 476 (n = 391 ZES, n = 85 BMS) patients whose volumetric intravascular ultrasound analyses were available at 8-month follow-up were studied. At 8 months, neointimal obstruction and maximum cross-sectional narrowing (CSN) were significantly lower in women than in men receiving ZES (neointimal obstruction 15.5 ± 9.5% vs 18.2 ± 10.9%, p = 0.025; maximum CSN 30.3 ± 13.2% vs 34.8 ± 15.0%, p = 0.007). Conversely, these parameters tended to be higher in women than in men receiving BMS (neointimal obstruction 36.3 ± 15.9% vs 27.5 ± 17.2%, p = 0.053; maximum CSN 54.3 ± 18.6% vs 45.6 ± 18.3%, p = 0.080). There was a significant interaction between stent type and gender regarding neointimal obstruction (p = 0.001) and maximum CSN (p = 0.003). Multivariate linear regression analysis revealed that female gender was independently associated with lower neointimal obstruction (p = 0.027) and maximum CSN (p = 0.004) for ZES but not for BMS. Compared to BMS, ZES were independently associated with a reduced risk for binary restenosis in both genders (odds ratio for women 0.003, p = 0.001; odds ratio for men 0.191, p <0.001), but the magnitude of this risk reduction with ZES was significantly greater in women than men (p = 0.015). In conclusion, female gender is independently associated with decreased neointimal hyperplasia in patients treated with ZES. The magnitude of risk reduction for binary restenosis with ZES is significantly greater in women than in men. © 2011 Elsevier Inc. All rights reserved. (Am J Cardiol 2011;108: 912–917)

The degree to which gender affects outcomes after percutaneous coronary intervention is still controversial. In patients treated with balloon angioplasty or bare-metal stents (BMS), inconclusive results have been obtained.[1–6] In patients treated with first-generation drug-eluting stents, including sirolimus-eluting stents (SES)[7] and paclitaxel-eluting stents (PES),[8] the risk for target lesion revascularization was similar between women and men after adjustment for clinical characteristics. However, in a pooled analysis of the Endeavor (Medtronic CardioVascular, Inc., Santa Rosa, California) zotarolimus-eluting stent (ZES) trials (ENDEAVOR I, ENDEAVOR II, ENDEAVOR II Continued Access Registry, and ENDEAVOR III), men had a 1.79-fold higher risk for target lesion revascularization than women by multivariate analysis.[9] To further elucidate this suggested gender difference, we compared vessel responses after ZES and BMS implantation in women and men using detailed intravascular ultrasound (IVUS) analysis.

Methods

The Endeavor ZES system is composed of the cobalt-chromium alloy Driver (Medtronic, Inc., Minneapolis, Minnesota) BMS, with a phosphorylcholine polymer that elutes zotarolimus. A dose concentration of 10 μg zotarolimus per 1 mm stent length, with 98% of zotarolimus elution within 14 days, provides treatment-level doses in the tissue for about 28 days after implantation. Several pivotal clinical trials evaluating the efficacy and safety of the ZES have been conducted. ENDEAVOR II, including the ENDEAVOR II Continued Access Registry, was a trial examining the safety and efficacy of ZES.[10,11] ENDEAVOR III[12] and ENDEAVOR IV[13] were also randomized trials comparing ZES with SES and PES, respectively. These trials used similar major inclusion and exclusion criteria as well as planned IVUS interrogation for all patients at prespecified enrollment sites after the procedure and at follow-up. The results of these trials have been described elsewhere.[14]

Data were obtained from the IVUS database of the Cardiovascular Core Analysis Laboratory at Stanford University (Stanford, California). Patients enrolled in ENDEAVOR II, ENDEAVOR II Continued Access Reg-

www.ajconline.org

Table 1
Baseline characteristics

Variable	ZES			BMS		
	Women (n = 110)	Men (n = 281)	p Value	Women (n = 18)	Men (n = 67)	p Value
Age (years)	64.4 ± 9.5	59.3 ± 10.7	<0.001	61.2 ± 8.8	58.5 ± 10.8	0.336
Hypertension	81.8%	65.6%	0.002	77.8%	54.5%	0.075
Diabetes mellitus	30.9%	19.9%	0.020	22.2%	11.9%	0.266
Hyperlipidemia	88.2%	82.5%	0.167	83.3%	82.1%	0.902
Current smoker	23.4%	25.3%	0.698	27.8%	29.9%	0.864
Family history	51.8%	41.5%	0.101	60.0%	32.3%	0.047
Previous myocardial infarction	19.3%	28.3%	0.067	27.8%	50.7%	0.083
Previous percutaneous coronary intervention	16.4%	24.9%	0.069	11.1%	19.7%	0.399

Data are expressed as mean ± SD or as percentages.

Table 2
Angiographic and procedural findings

Variable	ZES			BMS		
	Women (n = 110)	Men (n = 281)	p Value	Women (n = 18)	Men (n = 67)	p Value
Target coronary artery			0.534			0.734
Right coronary artery	24.5%	23.8%		33.3%	31.3%	
Left anterior descending	35.5%	37.4%		50.0%	43.3%	
Left circumflex	15.5%	19.9%		16.7%	25.4%	
Type of coronary lesion			0.668			0.311
A	5.5%	4.3%		5.6%	3.0%	
B1	29.1%	23.2%		22.2%	18.2%	
B2	40.9%	46.8%		27.8%	54.5%	
C	24.5%	25.7%		44.4%	24.2%	
B2/C	65.5%	72.5%	0.170	72.2%	78.8%	0.555
Pre–reference diameter (mm)	2.66 ± 0.40	2.77 ± 0.46	0.028	2.62 ± 0.34	2.91 ± 0.5	0.024
Pre–lesion length (mm)	13.99 ± 5.33	14.83 ± 6.05	0.202	14.59 ± 6.76	14.74 ± 5.39	0.924
Stent diameter (mm)	3.05 ± 0.33	3.11 ± 0.36	0.029	2.99 ± 0.33	3.19 ± 0.33	0.139
Total stent length (mm)	23.2 ± 7.4	23.0 ± 6.6	0.809	23.8 ± 5.1	22.9 ± 6.7	0.593

Data are expressed as mean ± SD or as percentages.

istry, ENDEAVOR III, and ENDEAVOR IV who were treated with ZES and had volumetric IVUS analysis available at 8-month follow-up were identified for study inclusion. Similarly, control subjects were patients in the ENDEAVOR II trial who were treated with the Driver BMS and had volumetric IVUS analysis available at 8-month follow-up.[10] There were no significant differences in baseline demographic and angiographic parameters before procedure between the IVUS[15–17] and total cohorts.[10,12,13] The protocol was approved by the institutional review board and written informed consent was obtained from each patient.

IVUS was performed in a standard fashion using an automated, motorized 0.5 mm/second pullback with a commercially available imaging system (40-MHz IVUS catheter, Boston Scientific Corporation, Natick, Massachusetts; or 20-MHz IVUS catheter, Volcano Corporation, Rancho Cordova, California) at baseline and 8-month follow-up. IVUS analysis was conducted in an independent core laboratory at Stanford University Medical Center (Cardiovascular Core Analysis Laboratory), and investigators were blinded to patient characteristics and randomization assignments. Volumetric measurements were performed using

software (echoPlaque; Indec Systems, Inc., Santa Clara, California), as previously described.[18] Volume index (volume [mm³]/length [mm]) was calculated for the vessel, plaque, neointima, stent, and lumen. Neointimal volume was then calculated as stent volume minus luminal volume, and neointimal obstruction was calculated as neointimal volume divided by stent volume (percent). Cross-sectional narrowing (CSN; percent) was defined as neointimal area divided by stent area. Incomplete stent apposition at baseline was defined as ≥1 stent strut clearly separated from the vessel wall with evidence of blood speckles behind the strut in a vessel segment not associated with any side branches.[19]

Categorical variables are expressed as frequency (percentage) and were compared using chi-square tests or Fisher's exact tests. Continuous variables are reported as mean ± SD and were compared using unpaired Student's t tests. Multiple linear regression analysis was used to determine the correlation of female gender with neointimal obstruction and maximum CSN. Multivariate logistic regression analysis was also performed to determine whether ZES were independently associated with a reduced risk for binary restenosis, defined as >50% diameter stenosis on angiography at 8-month follow-up. Variables with p values <0.20

Table 3

Intravascular ultrasound measurements at baseline and follow-up

Variable	ZES			BMS			p Value for Interaction
	Women	Men	p Value	Women	Men	p Value	
Baseline							
Vessel VI (mm³/mm)	12.5 ± 3.3	14.6 ± 4.3	0.001	13.9 ± 3.1	15.7 ± 4.2	0.232	
Plaque VI (mm³/mm)	5.7 ± 1.9	7.3 ± 2.7	<0.001	6.1 ± 2.0	7.7 ± 2.7	0.093	
Lumen VI (mm³/mm)	6.7 ± 1.9	7.4 ± 2.0	0.020	7.3 ± 1.9	8.1 ± 2.2	0.232	
Stent VI (mm³/mm)	6.7 ± 1.9	7.4 ± 2.0	0.017	7.4 ± 1.9	8.2 ± 2.2	0.235	
Minimum lumen area (mm²)	5.7 ± 1.7	6.1 ± 1.8	0.040	5.9 ± 1.6	6.8 ± 2.0	0.082	
Stent expansion ratio*	0.93 ± 0.15	0.95 ± 0.14	0.221	0.99 ± 0.16	0.96 ± 0.17	0.618	
Incomplete stent apposition	11.6%	19.3%	0.091	31.3%	17.7%	0.233	
Follow-up							
Vessel VI (mm³/mm)	12.9 ± 3.2	14.8 ± 4.2	<0.001	13.3 ± 3.5	15.8 ± 4.2	0.042	
Plaque VI (mm³/mm)	6.1 ± 1.8	7.8 ± 2.5	<0.001	6.0 ± 2.0	8.1 ± 2.8	0.013	
Lumen VI (mm³/mm)	5.8 ± 1.7	6.0 ± 1.8	0.415	4.3 ± 1.0	5.6 ± 2.0	<0.001	
Minimum lumen area (mm²)	4.7 ± 1.6	4.6 ± 1.7	0.884	3.0 ± 1.1	4.0 ± 1.8	0.024	
Neointimal obstruction (%)	15.5 ± 9.5	18.2 ± 10.9	0.025	36.3 ± 15.9	27.5 ± 17.2	0.053	0.001
Maximum CSN (%)	30.3 ± 13.2	34.8 ± 15.0	0.007	54.3 ± 18.6	45.6 ± 18.3	0.080	0.003
Incidence of maximum CSN ≥60%	1.8%	7.5%	0.032	33.3%	20.9%	0.269	0.026
Delta (follow-up minus baseline)							
Vessel VI (mm³/mm)	0.2 ± 0.9	0.1 ± 1.1	0.365	0.3 ± 0.8	0.2 ± 1.2	0.042	0.384
Plaque VI (mm³/mm)	0.1 ± 0.6	0.1 ± 1.0	0.983	0.3 ± 0.8	0.2 ± 0.8	0.013	0.365
Lumen VI (mm³/mm)	−0.9 ± 1.0	−1.4 ± 1.1	0.002	−3.0 ± 1.7	−2.4 ± 2.0	<0.001	0.051
Minimum lumen area (mm²)	−1.0 ± 1.1	−1.5 ± 1.2	0.002	−2.8 ± 1.9	−2.7 ± 1.8	0.833	0.023

Data are expressed as mean ± SD or as percentages.

VI = volume index.

* Defined as stent VI divided by manufacture's expected stent area.

Table 4

Correlation of female gender with neointimal obstruction and maximum cross-sectional narrowing by multivariate linear regression analysis

Stent Type	Neointimal Obstruction			Maximum CSN		
	Regression Coefficient	95% CI	p Value	Regression Coefficient	95% CI	p Value
ZES	−3.70	−6.97 to −0.43	0.027	−6.67	−11.23 to −2.10	0.004
BMS	10.74	−1.95 to 23.44	0.095	10.03	−3.78 to 23.86	0.151

Adjustment variables: age, hypertension, diabetes mellitus, hyperlipidemia, family history, history of myocardial infarction and percutaneous coronary intervention, type B2 or C lesion, and minimum lumen area at baseline.

CI = confidence interval.

on univariate analyses for ZES between the genders were inserted into these multivariate models after screening for multicollinearity.[20] Variables inserted into these models were age, hypertension, diabetes mellitus, hyperlipidemia, family history, history of myocardial infarction, previous percutaneous coronary intervention, type B2 or C lesion, and minimum lumen area at baseline. All tests were 2 sided, and statistical significance was defined as p <0.05. All analyses were performed using PASW Statistics version 18 (SPSS, Inc., Chicago, Illinois).

Results

We identified 391 patients with ZES and 85 patients with BMS meeting the inclusion criteria. The baseline clinical, angiographic, and procedural characteristics, stratified by gender and stent type, are listed in Tables 1 and 2. In the ZES group, women were significantly older and more likely to have hypertension, diabetes mellitus, and family histories of coronary heart disease but less likely to have histories of myocardial infarction and percutaneous coronary interven-

tion compared to men. Similar trends were seen in the BMS group (Table 1). Angiographically, women had significantly smaller preprocedural reference diameters than men, regardless of stent type. Otherwise, there were no significant differences in lesion location, lesion type, or lesion length between women and men in either group (Table 2).

At baseline, IVUS measurements in the ZES group, including vessel volume index, plaque volume index, luminal volume index, and minimum luminal area, were significantly smaller in women than men (Table 3). Similar trends were seen in the BMS group, although they were not statistically different. At 8 months, neointimal obstruction and maximum CSN were significantly lower in women compared to men receiving ZES (p = 0.025 and p = 0.007, respectively). Conversely, with BMS, these parameters tended to be higher in women than men (neointimal obstruction p = 0.053, maximum CSN p = 0.080). There was a significant interaction between gender and stent type in terms of neointimal obstruction (p = 0.001) and maximum CSN (p = 0.003). Likewise, the magnitude of change from
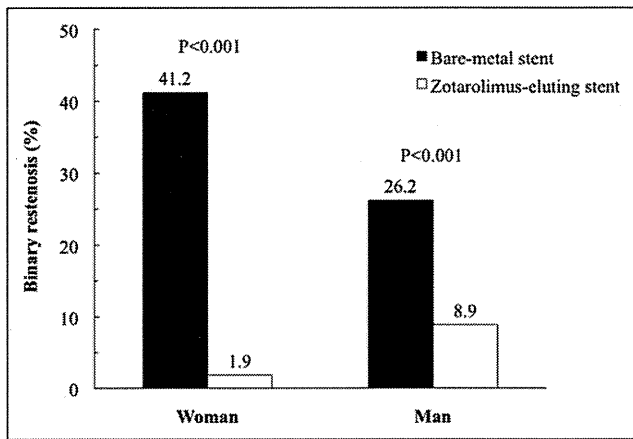
Figure 1. The rate of binary restenosis, defined as >50% diameter stenosis on angiography at 8-month follow-up, was significantly lower in patients treated with ZES than those with BMS in both genders.

follow-up to baseline in lumen volume index was significantly lower in women than men with ZES (p = 0.002), while it was higher in women than men with BMS (p < 0.001) (p for interaction = 0.051). After adjusting for clinical and angiographic differences in baseline characteristics, female gender was independently associated with a lower neointimal obstruction (p = 0.027) and maximum CSN (p = 0.004) in the ZES group but not in the BMS group (Table 4).

The incidence of binary restenosis at 8 months was significantly lower in the ZES group than the BMS group for both genders (Figure 1), and multivariate logistic regression analysis revealed that ZES were independently associated with a reduced risk for binary restenosis at 8 months for both genders (women: odds ratio 0.003, 95% confidence interval 0.000 to 0.105, p = 0.001; men: odds ratio 0.191, 95% confidence interval 0.076 to 0.479, p <0.001). However, the magnitude of risk reduction for binary restenosis with ZES was significantly greater in women than in men (p = 0.015).

Discussion

We investigated gender differences in IVUS parameters in women and men receiving ZES and BMS. Our study has 2 important findings. First, there was a significant interaction between gender and stent type, such that compared to men, women had significantly less neointimal hyperplasia with ZES at 8-month follow-up, independent of baseline clinical and angiographic characteristics. In contrast, women with BMS tended to have more neointimal hyperplasia than men, although this finding was no longer significant after adjusting for baseline characteristics. Second, women and men had a lower incidence and risk for binary restenosis at 8 months with ZES compared to BMS, but the magnitude of risk reduction of binary restenosis with ZES was significantly greater in women than men. Notably, these results also imply the opposite, that men had significantly more neointimal hyperplasia and less reduction in risk for binary restenosis with ZES than women at 8-month follow-up.

How gender differences affect outcomes for patients with symptomatic coronary artery disease is an ongoing issue. In patients treated with balloon angioplasty or BMS, inconsistent observations for restenosis or repeat revascularization between the genders have been reported. Some reports have shown that women have worse outcomes after BMS implantation,[1,2] whereas others have suggested that men have worse outcomes than women when treated with balloon angioplasty[3] and BMS[4]. There are also data showing no difference in the rate of restenosis or target lesion revascularization between the genders.[5,6] In the present study, neointimal obstruction and maximum CSN tended to be higher in women compared to men receiving BMS, but this difference was attenuated after adjusting for baseline clinical and angiographic characteristics, suggesting an absence of gender differences with respect to neointimal hyperplasia after BMS implantation. A single explanation for these inconsistent findings in the published research is lacking, but several possibilities exist. First, although patients who underwent percutaneous coronary intervention were registered consecutively, the percentage of women enrolled in each study varied, ranging from 15%[2] to 55%,[5] suggesting that variable rates of selection bias may have existed at the time of enrollment. Second, disparities in secondary prevention implementation, with women being less likely than men to receive optimal medical therapy including statins, aspirin, and β blockers,[21] may affect results depending on the study location or protocol. Finally, there is a tendency for women to be treated with medical therapy rather than repeat revascularization after a procedure, especially in registry data, because of older age and greater risk profiles,[21] which could skew the data from treatment bias.[22–24] These statistical biases and treatment differences between the genders may help explain variable outcomes between women and men after BMS implantation.

Data regarding gender differences with drug-eluting stents have also been inconsistent. No significant gender differences were found in the adjusted risk for target lesion revascularization in patients treated with the first-generation PES and SES. Lansky et al[8] investigated gender-based outcomes in 662 patients with PES. In their results, although the rate of target lesion revascularization at 1 year was significantly higher in women than in men (7.6% vs 3.2%, p = 0.03), the risk for target lesion revascularization for women at 1 year became insignificant after adjusting for baseline differences, including age, reference diameter, and lesion length (adjusted hazard ratio 1.72, 95% confidence interval 0.69 to 4.37, p = 0.25), suggesting that the higher incidence of target lesion revascularization in women compared to men was not related to gender itself but rather to the influence of smaller vessels and longer lesions in women. Solinas et al[7] examined cardiac events in 878 patients with SES derived from 4 clinical randomized trials (RAVEL, SIRIUS, E-SIRIUS, and C-SIRIUS). They found that the target lesion revascularization rate did not differ between women and men (4.1% vs 4.3%, p = 0.86) and that female gender was not an independent predictor of target lesion revascularization by multivariate analysis (hazard ratio 0.63, 95% confidence interval 0.25 to 1.53, p = 0.31). In contrast, in a pooled analysis of the Endeavor ZES, Mehta et al[9] investigated 1,306 patients and found that men

had a 1.79-fold higher risk for target lesion revascularization compared to women by multivariate analysis. More recently, Brown et al[25] also showed a trend toward higher target lesion revascularization at 2 years in men than women (8.2% vs 7.9%, p = 0.07) in the 6 pivotal clinical trials of Endeavor ZES. Consistent with these reports, our study found that female gender was associated with decreased neointimal growth after ZES implantation, independent of clinical and angiographic characteristics such as age, cardiac risk factors, history of myocardial infarction and percutaneous coronary intervention, and lesion diameter and morphology. Furthermore, there was a significant interaction between stent type and gender with respect to neointimal hyperplasia. Compared to men, women had greater neointimal growth with BMS and less neointimal growth with ZES, whereas men compared to women had less neointimal growth with BMS but greater neointimal growth with ZES. Although we cannot argue a cause-effect relation between neointimal growth and stent components in this study, it is possible that the stent itself, or stent additives, such as zotarolimus and/or the phosphorylcholine polymer, affect the difference in neointimal growth between the genders. It is unknown why gender differences in neointimal hyperplasia were observed with ZES but not with SES or PES. In the present study, the overall neointimal obstruction for ZES was 17.5%, whereas neointimal obstruction for SES and PES was 2.7%[16] and 9.9%,[17] respectively. Relatively greater neointimal proliferation for ZES compared to SES and PES might be a possible explanation. As such, IVUS resolution may be insufficient to detect gender differences in neointimal hyperplasia when the amount of neointimal proliferation is small. It is possible that different stent materials have variable effects in women and men, with some materials resulting in no difference and others causing significant clinical differences between the genders. With ZES having the shortest duration of drug presence after implantation among ZES,[14.26] SES,[27,28] and PES,[29] it may also be that the length of drug exposure is more important in men than in women, whereby men need a longer duration of drug elution to fully suppress neointimal growth. It is also speculated that men may need a higher amount of drug dose to achieve sufficient neointimal suppression.

Regarding the efficacy of ZES, the incidence of binary restenosis at 8 months was significantly lower with ZES than BMS for both genders in the present study, suggesting that ZES have a beneficial effect on neointimal suppression compared to BMS, independent of gender. Previous drug-eluting stent trials, including SES and PES, also showed that the magnitude of restenosis reduction compared to BMS was similar between the genders.[6-8.30] However, in the present study, the magnitude of risk reduction for binary restenosis at 8 months in patients with ZES versus BMS was significantly greater in women than in men. Although the exact reason for this observation of ZES is not clear, vascular responses to the stent and its added materials may again play a role.

We should note several limitations of this study. First, selection bias might be present because of the post hoc analysis setting design. However, clinical trials using similar inclusion and exclusion criteria were used in our study.

In addition, there were no differences in baseline demographic and angiographic parameters before the procedure between the IVUS and total cohorts. Therefore, selection bias may be minimal. Second, the IVUS follow-up period was relatively short. Further long-term study will be needed to confirm these findings. Third, the number of patients in the BMS group was relatively small compared to the ZES group. Regarding overall cases enrolled in this study, the number of women was relatively small compared to men.

1. Kishi K, Hiasa Y, Suzuki N, Takahashi T, Hosokawa S, Tanimoto M, Otani R. Predictors of recurrent restenosis after coronary stenting: an analysis of 197 patients. *J Invasive Cardiol* 2002;14:187–191.
2. Trabattoni D, Bartorelli AL, Montorsi P, Fabbiocchi F, Loaldi A, Galli S, Ravagnani P, Cozzi S, Grancini L, Liverani A, Leon ME, Robertson C, Boyle P. Comparison of outcomes in women and men treated with coronary stent implantation. *Catheter Cardiovasc Interv* 2003;58:20–28.
3. Arnold AM, Mick MJ, Piedmonte MR, Simpfendorfer C. Gender differences for coronary angioplasty. *Am J Cardiol* 1994;74:18–21.
4. Mehilli J, Kastrati A, Bollwein H, Dibra A, Schuhlen H, Dirschinger J, Schomig A. Gender and restenosis after coronary artery stenting. *Eur Heart J* 2003;24:1523–1530.
5. Fishman RF, Kuntz RE, Carrozza JP Jr, Friedrich SP, Gordon PC, Senerchia CC, Baim DS. Acute and long-term results of coronary stents and atherectomy in women and the elderly. *Coron Artery Dis* 1995;6:159–168.
6. Abbott JD, Vlachos HA, Selzer F, Sharaf BL, Holper E, Glaser R, Jacobs AK, Williams DO. Gender-based outcomes in percutaneous coronary intervention with drug-eluting stents (from the National Heart, Lung, and Blood Institute Dynamic Registry). *Am J Cardiol* 2007;99:626–631.
7. Solinas E, Nikolsky E, Lansky AJ, Kirtane AJ, Morice MC, Popma JJ, Schofer J, Schampaert E, Pucelikova T, Aoki J, Fahy M, Dangas GD, Moses JW, Cutlip DE, Leon MB, Mehran R. Gender-specific outcomes after sirolimus-eluting stent implantation. *J Am Coll Cardiol* 2007;50:2111–2116.
8. Lansky AJ, Costa RA, Mooney M, Midei MG, Lui HK, Strickland W, Mehran R, Leon MB, Russell ME, Ellis SG, Stone GW. Gender-based outcomes after paclitaxel-eluting stent implantation in patients with coronary artery disease. *J Am Coll Cardiol* 2005;45:1180–1185.
9. Mehta RH, Leon MB, Sketch MH Jr. The relation between clinical features, angiographic findings, and the target lesion revascularization rate in patients receiving the Endeavor zotarolimus-eluting stent for treatment of native coronary artery disease: an analysis of ENDEAVOR I, ENDEAVOR II, ENDEAVOR II Continued Access Registry, and ENDEAVOR III. *Am J Cardiol* 2007;100(suppl):62M–70M.
10. Fajadet J, Wijns W, Laarman GJ, Kuck KH, Ormiston J, Munzel T, Popma JJ, Fitzgerald PJ, Bonan R, Kuntz RE. Randomized, double-blind, multicenter study of the Endeavor zotarolimus-eluting phosphorylcholine-encapsulated stent for treatment of native coronary artery lesions: clinical and angiographic results of the ENDEAVOR II trial. *Circulation* 2006;114:798–806.
11. Schultheiss HP, Grube E, Kuck KH, Suttorp MJ, Heuer H, Bonnier H, Popma JJ, Kuntz RE, Fadajet J, Wijns W. Safety of direct stenting with

the Endeavor stent: results of the Endeavor II continued access registry. *Eurointervention* 2007;3:76–81.

12. Kandzari DE, Leon MB, Popma JJ, Fitzgerald PJ, O'Shaughnessy C, Ball MW, Turco M, Applegate RJ, Gurbel PA, Midei MG, Badre SS, Mauri L, Thompson KP, LeNarz LA, Kuntz RE. Comparison of zotarolimus-eluting and sirolimus-eluting stents in patients with native coronary artery disease: a randomized controlled trial. *J Am Coll Cardiol* 2006;48:2440–2447.

13. Leon MB, Mauri L, Popma JJ, Cutlip DE, Nikolsky E, O'Shaughnessy C, Overlie PA, McLaurin BT, Solomon SL, Douglas JS Jr, Ball MW, Caputo RP, Jain A, Tolleson TR, Reen BM III, Kirtane AJ, Fitzgerald PJ, Thompson K, Kandzari DE. A randomized comparison of the ENDEAVOR zotarolimus-eluting stent versus the TAXUS paclitaxel-eluting stent in de novo native coronary lesions 12-month outcomes from the ENDEAVOR IV trial. *J Am Coll Cardiol* 2010;55:543–554.

14. Pinto Slottow TL, Waksman R. Overview of the 2007 Food and Drug Administration circulatory system devices panel meeting on the Endeavor zotarolimus-eluting coronary stent. *Circulation* 2008;117:1603–1608.

15. Sakurai R, Hongo Y, Yamasaki M, Honda Y, Bonneau HN, Yock PG, Cutlip D, Popma JJ, Zimetbaum P, Fajadet J, Kuntz RE, Wijns W, Fitzgerald PJ. Detailed intravascular ultrasound analysis of zotarolimus-eluting phosphorylcholine-coated cobalt-chromium alloy stent in de novo coronary lesions (results from the ENDEAVOR II trial). *Am J Cardiol* 2007;100:818–823.

16. Miyazawa A, Ako J, Hongo Y, Hur SH, Tsujino I, Courtney BK, Hassan AH, Kandzari DE, Honda Y, Fitzgerald PJ. Comparison of vascular response to zotarolimus-eluting stent versus sirolimus-eluting stent: intravascular ultrasound results from ENDEAVOR III. *Am Heart J* 2008;155:108–113.

17. Waseda K, Miyazawa A, Ako J, Hasegawa T, Tsujino I, Sakurai R, Yock PG, Honda Y, Kandzari DE, Leon MB, PJ F. Intravascular ultrasound results from the ENDEAVOR IV trial: randomized comparison between zotarolimus- and paclitaxel-eluting stents in patients with coronary artery disease. *J Am Coll Cardiol Intv* 2009;8:779–784.

18. Kataoka T, Grube E, Honda Y, Morino Y, Hur SH, Bonneau HN, Colombo A, Di Mario C, Guagliumi G, Hauptmann KE, Pitney MR, Lansky AJ, Stertzer SH, Yock PG, Fitzgerald PJ. 7-hexanoyltaxol-eluting stent for prevention of neointimal growth: an intravascular ultrasound analysis from the Study to Compare Restenosis Rate Between Quest and Quads-QP2 (SCORE). *Circulation* 2002;106:1788–1793.

19. Honda Y. Drug-eluting stents. Insights from invasive imaging technologies. *Circ J* 2009;73:1371–1380.

20. Slinker BK, Glantz SA. Multiple linear regression: accounting for multiple simultaneous determinants of a continuous dependent variable. *Circulation* 2008;117:1732–1737.

21. Crilly M, Bundred P, Hu X, Leckey L, Johnstone F. Gender differences in the clinical management of patients with angina pectoris: a cross-sectional survey in primary care. *BMC Health Serv Res* 2007;7:142.

22. Jneid H, Fonarow GC, Cannon CP, Hernandez AF, Palacios IF, Maree AO, Wells Q, Bozkurt B, Labresh KA, Liang L, Hong Y, Newby LK, Fletcher G, Peterson E, Wexler L. Sex differences in medical care and early death after acute myocardial infarction. *Circulation* 2008;118:2803–2810.

23. Daly C, Clemens F, Lopez Sendon JL, Tavazzi L, Boersma E, Danchin N, Delahaye F, Gitt A, Julian D, Mulcahy D, Ruzyllo W, Thygesen K, Verheugt F, Fox KM. Gender differences in the management and clinical outcome of stable angina. *Circulation* 2006;113:490–498.

24. Novack V, Cutlip DE, Jotkowitz A, Lieberman N, Porath A. Reduction in sex-based mortality difference with implementation of new cardiology guidelines. *Am J Med* 2008;121:597–603.

25. Brown RA, Williams M, Barker CM, Mauri L, Meredith IT, Fajadet J, Wijns W, Leon MB, Kandzari DE. Sex-specific outcomes following revascularization with zotarolimus-eluting stents: comparison of angiographic and late-term clinical results. *Catheter Cardiovasc Interv* 2010;76:804–813.

26. Chen YW, Smith ML, Sheets M, Ballaron S, Trevillyan JM, Burke SE, Rosenberg T, Henry C, Wagner R, Bauch J, Marsh K, Fey TA, Hsieh G, Gauvin D, Mollison KW, Carter GW, Djuric SW. Zotarolimus, a novel sirolimus analogue with potent anti-proliferative activity on coronary smooth muscle cells and reduced potential for systemic immunosuppression. *J Cardiovasc Pharmacol* 2007;49:228–235.

27. Sousa JE, Costa MA, Abizaid AC, Rensing BJ, Abizaid AS, Tanajura LF, Kozuma K, Van Langenhove G, Sousa AG, Falotico R, Jaeger J, Popma JJ, Serruys PW. Sustained suppression of neointimal proliferation by sirolimus-eluting stents: one-year angiographic and intravascular ultrasound follow-up. *Circulation* 2001;104:2007–2011.

28. Klugherz BD, Llanos G, Lieuallen W, Kopia GA, Papandreou G, Narayan P, Sasseen B, Adelman SJ, Falotico R, Wilensky RL. Twenty-eight-day efficacy and phamacokinetics of the sirolimus-eluting stent. *Coron Artery Dis* 2002;13:183–188.

29. Silber S, Grube E. The Boston Scientific antiproliferative, paclitaxel eluting stents (TAXUS). In: Serruys P, Kutryk M, eds. Handbook of Coronary Stents. 4th ed. London, UK: Martin Dunitz Publishers Ltd; 2001:311–319.

30. Lansky AJ, Hochman JS, Ward PA, Mintz GS, Fabunmi R, Berger PB, New G, Grines CL, Pietras CG, Kern MJ, Ferrell M, Leon MB, Mehran R, White C, Mieres JH, Moses JW, Stone GW, Jacobs AK. Percutaneous coronary intervention and adjunctive pharmacotherapy in women: a statement for healthcare professionals from the American Heart Association. *Circulation* 2005;111:940–953.